

Spatially resolved characterization of InGaAs/GaAs quantum dot structures by scanning spreading resistance microscopy

T. Hakkarainen,^{1,a)} O. Douhéret,^{1,b)} S. Anand,^{1,c)} L. Fu,^{2,d)} H. H. Tan,² and C. Jagadish²

¹*Division of Semiconductor Materials, School of Information and Communication Technology, Royal Institute of Technology, Electrum 229, 16440 Kista, Sweden*

²*Department of Electronic Materials Engineering, Research School of Physics and Engineering, The Australian National University, Canberra ACT 0200, Australia*

(Received 1 March 2010; accepted 29 June 2010; published online 27 July 2010)

Cross-sectional scanning spreading resistance microscopy (SSRM) is used to investigate stacked InGaAs/GaAs quantum dot (QD) structures with different doping schemes. Spatially resolved imaging of the QDs by SSRM is demonstrated. The SSRM contrast obtained for the QD layers is found to depend on doping in the structure. In the undoped structures both QD-layers and QDs within the layers could be resolved, while in the doped structures the QD layers appear more or less uniformly broadened. The origin of the SSRM contrast in the QD layer in the different samples is discussed and correlated with doping schemes. © 2010 American Institute of Physics.

[doi:10.1063/1.3467138]

In recent years substantial research effort has been made on employing quantum dot (QD) structures in optoelectronic devices such as lasers and photodetectors. Applications based on QDs invariably depend on the particular QD properties and are often tailored for the specific purpose. Apart from the desired wavelength of operation, an important aspect for devices such as QD infrared photodetectors (QDIPs) (Refs. 1–3) is doping, and has received much attention. In practice, doping can be realized either by introducing a modulation-doped layer at a short distance from the QDs, or, by directly doping the dot-layer during growth and/or by doping only the barriers. Doping via the first method is relatively difficult to control, while the latter method allows for better control but can also degrade the optical quality of the QDs.^{4,5} In addition the presence of dopants in the dots or barriers may also affect the dot density, average size, and size distribution.^{6,7} In this context, the way doping schemes are implemented can have implications on the device performance and a good understanding of the electrical properties of the QD structures is necessary. Further, since the active region of the device consists of structures with nanoscale dimensions (QDs and barrier layer thickness) it becomes essential to investigate the utility of electrical characterization techniques that can also provide nanoscale spatial resolution.

Atomic force microscopy (AFM) based techniques such as scanning capacitance microscopy (SCM)⁸ and scanning spreading resistance microscopy (SSRM)⁹ have emerged as powerful methods to map electrical properties of semiconductor devices with high spatial resolution. More recently, profiling of carriers in InGaAs/InP quantum wells (QWs) by SCM¹⁰ and SSRM¹¹ has been demonstrated. Investigations using specially designed QW structures have demonstrated that SSRM with commercial probes has superior

resolution—sub-5 nm as compared to about 30 nm with SCM.¹² Although the potential of SCM for characterizing QD structures has been recognized the measurements were severely limited by contrast reversal caused by surface/interface states.¹³ In this work cross-sectional SSRM is used to investigate InGaAs/GaAs QD structures with different doping schemes, and thereby to establish the potential of SSRM for characterizing such structures.

In_{0.5}Ga_{0.5}As self-organized QD structures were grown in Stranski–Krastanow growth mode on n⁺GaAs substrates using metal organic chemical vapor deposition. After deposition of 500 nm n-doped ($1 \times 10^{18} \text{ cm}^{-3}$) GaAs, five layers of InGaAs QDs were grown separated by 50 nm thick GaAs barriers. The samples were then covered with a 500 nm thick n-GaAs ($1 \times 10^{18} \text{ cm}^{-3}$) cap layer. The grown structures were either undoped (nonintentionally doped) or n-type (Si donor). In order to study the effects of doping on the QDs, three different doping schemes were employed—(i) sample A was undoped (reference); (ii) sample B was with doped QD layers and undoped GaAs barriers; and (iii) sample C was with undoped QD layers but the GaAs barriers were doped. In samples B and C, Si was introduced during the growth to result in a nominal concentration of $1 \times 10^{17} \text{ cm}^{-3}$. AFM of uncapped structures with a single QD layer shows QDs with typical sizes of 20–30 nm diameter and 3–5 nm height. However, the QD density was higher ($\sim 7 \times 10^{10} \text{ cm}^{-2}$) when the QD layer was doped compared to that in undoped samples ($\sim 5 \times 10^{10} \text{ cm}^{-2}$).

The SSRM measurements were carried out using Digital Instrument's Nanoscope Dimension 3100 microscope equipped with spreading resistance measurement electronics. SSRM is an AFM-based technique in which the local resistance of the surface/near surface region of the sample is obtained from the electrical current flowing between a conductive-tip and the sample that is biased relative to the tip. A two-dimensional map of the resistance is obtained by scanning the probe over the sample surface, for instance its cross-section. The QD sample was cross-sectioned by manually cleaving the sample in ambient air and a back Ohmic contact was provided. No special chemical treatment

^{a)}Permanent address: Department of Micro and Nanosciences, School of Science and Technology, Aalto University, P.O. Box 13500, 00076 Aalto, Finland.

^{b)}Present address: Service for Chemistry of Novel Materials, Materia-Nova, Mons University, Mons, Belgium.

^{c)}Electronic mail: anand@kth.se.

^{d)}Electronic mail: ful109@physics.anu.edu.au.

(passivation) was performed after cleaving. The SSRM probes used were commercial B-doped diamond coated Si tips with a force constant of ~ 40 N/m (Nanosensors GmbH) and the average tip diameter is of the order of 30 nm. However, the actual contact could be much smaller due to the presence of diamond nanocrystallites in the coating. The current was measured using a logarithmic amplifier and the dc bias was applied to the sample. The scan rate was 1 Hz in all the measurements. To achieve highest possible resolution the scanning was conducted at the lowest deflection possible, still maintaining a stable contact. The best conditions for imaging the QD samples were obtained for 0.5 to 1 V and 0.2 to 0.5 V for the sample (reverse) bias and deflection set-point, respectively.

It is known that for III–V materials the tip-sample contact is Schottky-like and thus the currents measured in SSRM depend on the local Schottky-barrier height which is material dependent and on the doping.^{9,11,14} Current-voltage measurements performed (not shown) at single points (stationary probe) on GaAs substrate region showed Schottky-like characteristics, in agreement with similar SSRM measurements reported earlier for GaAs and InP.¹⁴ For n-GaAs and n-InGaAs typical values of 900 meV and 200–300 meV (Ref. 15) for the Schottky barrier heights (macroscopic contacts) have been reported, respectively. However, in the present case the In(Ga)As QDs are embedded in GaAs. Thus when the tip is in contact with a QD, the effective barrier height includes the conduction band offset between the dot and the barrier. For InAs/GaAs a value of 200 meV has been measured¹⁶ and a similar value has been suggested for $\text{In}_{0.5}\text{Ga}_{0.5}\text{As}/\text{GaAs}$ dots.¹⁷ Taking this into account, the effective barrier height for the dot can be estimated to be approximately in the 400–500 meV range, which is still significantly lower compared to that of GaAs. Thus the SSRM contrast (current) is primarily determined by the surface properties of the material; higher currents will be obtained in the InGaAs QD regions compared to the GaAs regions. The ground state energy level of the wetting layer lies closer to the GaAs barrier edge, which would result in a low density of accumulated electrons, especially since most of the electrons transferred from the GaAs barrier will be in the dots. Therefore, the current conduction via the wetting layer may be expected to be low except perhaps when this layer is also doped (as in the dot-doped sample).

Figure 1 shows SSRM images and current-profiles obtained for the undoped sample (A). The QD layers are clearly visible in the images [Figs. 1(a) and 1(b)], appearing bright compared to the (dark) barrier regions. The average value of the current in the reference layers (doped GaAs buffer and cap layers) is about $2 \mu\text{A}$. Compared to this significantly lower values (0.1–0.2 μA) are seen for the nominally undoped GaAs-barrier layers. Thus the measured currents are qualitatively consistent with the doping levels in the different GaAs regions. Due to the lower Schottky barrier height, hence lower contact resistance, the current in the vicinity of QDs shows the expected spike [Figs. 1(c) and 1(d)] due to higher current flow with respect to the surroundings; the bright spots (Fig. 1(b)) correspond to individual InGaAs QDs. Figure 1(e) shows a zoomed image of Fig. 1(b) to illustrate imaging of individual dots. The measured width (50 nm) of the GaAs barrier layers [Fig. 1(c)] is consistent with growth. The measured average separation [Fig. 1(d)] of the

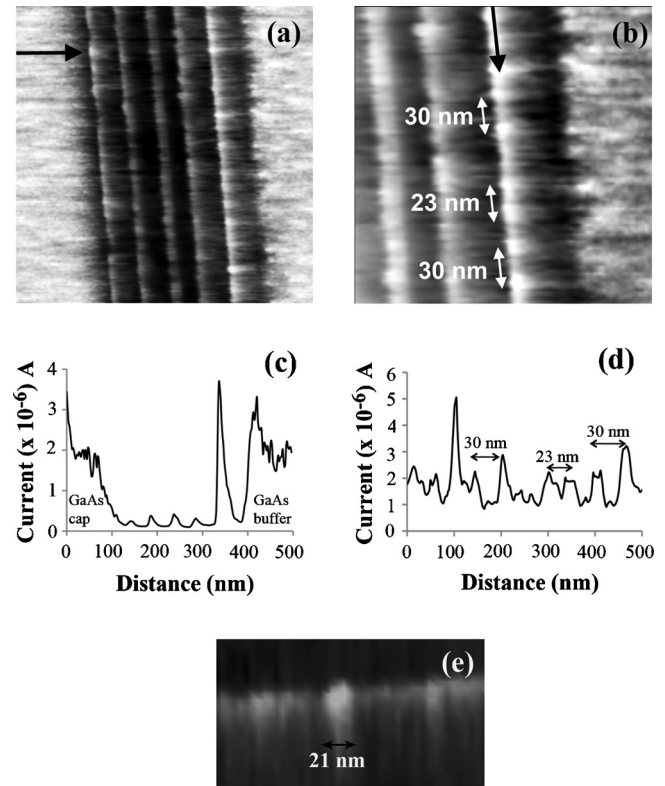


FIG. 1. SSRM images of the undoped sample (sample A). (a) Current image obtained at 0.5 V sample bias (i.e., reverse bias condition) clearly showing the five QD layers. The buffer and cap GaAs layers are in the right and left side of the QD layers, respectively. The image size is $500 \times 500 \text{ nm}^2$. The arrow points the location along which the horizontal line profile shown in (c) was taken. (b) $250 \times 250 \text{ nm}^2$ image showing bright current spots corresponding to QDs. The distances between some of the QDs are marked. The line profile shown in (d) was taken along the QD layer pointed by the arrow. (e) Close-up image of one of the QDs; the imaged diameter is about 20 nm.

resolved dots in the rightmost QD layer is ~ 25 nm and is consistent with that estimated from the QD density independently obtained by AFM on an uncapped dot sample. In the middle layers the QDs are less resolved and also currents are lower. The higher currents in the outer QD layers could be due to the proximity of the highly doped GaAs contact layers. This is supported by the results [Figs. 2(a) and 2(b)] obtained for the doped samples, wherein the QD layers show similar contrast. This result confirms that in some of the QDIPs which employ undoped QDs as active layers, in addition to background doping in the structure, the highly doped contact layers also act as important carrier supplier for the operation of the devices.¹ The average width of the peaks in Fig. 1(d) is about 20 nm in good agreement with the independently measured dot diameters (AFM). However, in the scan direction (across the layers) the spatial resolution is not as high. The average full-width-at-half maximum of the current peaks at the QD layers [Fig. 1(c)] is 16 nm which is about four times larger than the height of the QDs. This suggests that when the tip is in the GaAs barrier region adjacent to the Q-dot there is a path for current flow from the tip. Such a widening has earlier been observed in SSRM imaging of QWs under reverse bias conditions and attributed to a tunneling effect.¹¹ It is reasonable to assume the same effect being responsible for the widening observed here.

Figure 2 shows the SSRM images and current profiles obtained for the doped samples (B and C). As seen from

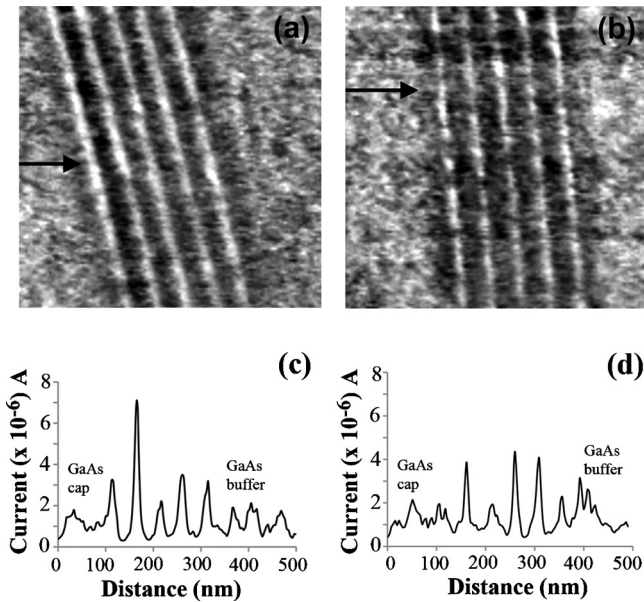


FIG. 2. SSRM images (a) and (b) of the dot-doped (sample B) and of the barrier-doped (sample C) samples, respectively. The images are $500 \times 500 \text{ nm}^2$ in size and were taken with a sample bias of 1 V (i.e., reverse bias condition). The corresponding horizontal line profiles taken along the position indicated by the arrows are shown in (c) and (d).

Fig. 2, the QD layers are clearly distinguishable by the bright contrast and spaced by 50 nm. In both samples B and C the (average) current is about $1\text{--}2 \mu\text{A}$ in the reference layers, consistent with that obtained for sample A [Fig. 1(c)]. However, due to the higher doping in these samples the measured current is higher for the GaAs-barrier layers compared to the undoped case (sample A). In sample C [Fig. 2(d)] consistent with the lower doping (10^{17} cm^{-3}) the currents ($0.58\text{--}0.8 \mu\text{A}$) are also lower compared to the reference layers. Similarly in sample B, the currents ($0.2\text{--}0.3 \mu\text{A}$) in the barriers is lower and is comparable to the values obtained for sample A with undoped barriers. In sample B, the doping in the dot layers should provide increased conduction, while in sample C one has the transfer of carriers from the barriers which increases the conductivity of the QD layers. Consistent with this the average current in the QD-layers in both doped samples [Figs. 2(c) and 2(d)] is about a few microamperes which is appreciably higher compared to the undoped sample A.

Since the widths of the current peaks [Figs. 2(c) and 2(d)] are comparable to that obtained for sample A, the spatial resolution in the scan direction is similar. Although the presence of current spots along the dot layers can also be noted, the resolution and contrast is poor compared to that obtained for sample A (Fig. 1). It appears to be more or less continuously broadened for sample B [Fig. 2(a)], suggesting increased density of dots. Si atoms have been reported to act as nucleation centers during the growth of QDs, affecting the dot density and resulting in larger size inhomogeneity.^{6,7} This could, in part, explain the trend observed here. For sample C, although only the barrier is doped, most likely it affects the surface energy in which the subsequent QDs are deposited and thus the dot density. These arguments together with the

contrast seen for sample C [Fig. 2(b)] suggest a lower QD density for sample C. Nevertheless, for sample B an estimate of $\sim 20 \text{ nm}$ for interdot spacing is made from the density ($7 \times 10^{10} \text{ cm}^{-2}$) obtained from AFM measurements of uncapped but doped dot samples. Thus increased density by itself cannot fully explain the results for the doped samples. The situation is more complex with parallel conduction in the wetting layer and contributions coming from subsurface dots.

In summary, SSRM was used to investigate stacked InGaAs/GaAs QD structures with different doping schemes. It was demonstrated that SSRM is capable of detecting and resolving QDs in the dot layers with nanoscale spatial resolution. The undoped sample provided the best resolution and contrast while the dot layers in the doped samples appeared more or less continuously broadened. The origin of the SSRM contrast and the spatial resolution in the QD layers in the different samples was addressed and the results were correlated with the doping in the structure and the effects of doping on QD density. It shows that this technique could provide important insight into the operation mechanism of QD-based optoelectronic devices such as QDIP.

T. Hakkarainen, O. Douhéret, and S. Anand would like to acknowledge the Swedish Research Council (VR) for financial support and the Kurt-Alice Wallenberg (KAW) foundation for financing the microscope. L. Fu, H. H. Tan, and C. Jagadish would like to acknowledge the Australian Research Council (ARC) for financial support and Australian National Fabrication Facility (ANFF) for access to the facilities.

- ¹L. Fu, P. Lever, K. Sears, H. H. Tan, and C. Jagadish, *IEEE Electron Device Lett.* **26**, 628 (2005).
- ²V. Ryzhii, I. Khmyrova, M. Ryzhii, and V. Mitin, *Semicond. Sci. Technol.* **19**, 8 (2004).
- ³S. Chakrabarti, A. D. Stiff-Roberts, P. Bhattacharya, and S. W. Kennerly, *J. Vac. Sci. Technol. B* **22**, 1499 (2004).
- ⁴J. Phillips, K. Kamath, X. Zhou, N. Chervela, and P. Bhattacharya, *J. Vac. Sci. Technol. B* **16**, 1343 (1998).
- ⁵H. L. Wang, F. H. Yang, and S. L. Feng, *J. Cryst. Growth* **212**, 35 (2000).
- ⁶Z. Qian, F. Songlin, N. Dong, Z. Haijun, W. Zhiming, and D. Yuanming, *J. Cryst. Growth* **200**, 603 (1999).
- ⁷Y. M. Park, Y. J. Park, K. M. Kim, J. I. Lee, and K. H. Yoo, *Physica E* **25**, 647 (2005).
- ⁸C. C. Williams, *Annu. Rev. Mater. Sci.* **29**, 471 (1999).
- ⁹P. De Wolf, M. Geva, T. Hantschel, W. Vandervost, and R. B. Bylisma, *Appl. Phys. Lett.* **73**, 2155 (1998).
- ¹⁰K. Maknys, O. Douhéret, and S. Anand, *Appl. Phys. Lett.* **83**, 4205 (2003).
- ¹¹K. Maknys, O. Douhéret, and S. Anand, *Appl. Phys. Lett.* **83**, 2184 (2003).
- ¹²O. Douhéret, S. Bonsels, and S. Anand, *J. Vac. Sci. Technol. B* **23**, 61 (2005).
- ¹³Z. Y. Zhao, W. M. Zhang, C. Yi, A. D. Stiff-Roberts, B. J. Rodriguez, and A. P. Baddorf, *Appl. Phys. Lett.* **92**, 092101 (2008).
- ¹⁴R. P. Lu, K. L. Kavanagh, St. J. Dixon-Warren, A. J. SpringThorpe, R. Streater and I. Calder, *J. Vac. Sci. Technol. B* **20**, 1682 (2002).
- ¹⁵K. Kajiyama, Y. Mizushima, and S. Sakata, *Appl. Phys. Lett.* **23**, 458 (1973).
- ¹⁶C. M. A. Kapteyn, F. Heinrichsdorff, O. Stier, R. Heitz, M. Grundmann, N. D. Zakharov, D. Bimberg, and P. Werner, *Phys. Rev. B* **60**, 14265 (1999).
- ¹⁷Z. Q. Fang, Q. H. Xie, D. C. Look, J. Ehret, and J. E. Van Nostrand, *J. Electron. Mater.* **28**, L13 (1999).